Conference on Modelling Fluid Flow (CMFF'25)
The 19th International Conference on Fluid Flow Technologies
Budapest, Hungary, August 26-August 29, 2025

SPHERICAL STABILITY AND BREAKUP LIMIT OF OSCILLATING MICROBUBBLES

Dániel NAGY[1], Péter KALMÁR[2], Kálmán KLAPCSIK[3], Ferenc HEGEDŰS[4]

[1] Department of Hydrodynamic Systems, Faculty of Mechanical Engineering, Budapest University of Technology and Economics. Muegyetem rakpart 3, H-1111 Budapest, Hungary. E-mail: dnagy@hds.bme.hu
[2] Department of Hydrodynamic Systems, Faculty of Mechanical Engineering, Budapest University of Technology and Economics. Muegyetem rakpart 3, H-1111 Budapest, Hungary. E-mail: pkalmar@hds.bme.hu
[3] Department of Hydrodynamic Systems, Faculty of Mechanical Engineering, Budapest University of Technology and Economics. Muegyetem rakpart 3, H-1111 Budapest, Hungary. E-mail: kklapcsik@hds.bme.hu
[4] Corresponding Author. Department of Hydrodynamic Systems, Faculty of Mechanical Engineering, Budapest University of Technology and Economics. Muegyetem rakpart 3, H-1111 Budapest, Hungary. E-mail: fhegedus@hds.bme.hu

ABSTRACT

This study investigates the spherical stability and breakup limits of oscillating microbubbles in an acoustic standing wave, employing both a Reduced Order Model (ROM) and a multiphase flow solver. The ROM couples the spherical bubble dynamics, governed by the Keller-Miksis equation, with axisymmetric surface mode oscillations, formulated as a system of ordinary differential equations. The results from the ROM are compared against multiphase CFD simulations performed using the ALPACA flow solver. While multiphase CFD simulations are computationally more intensive, they offer deeper insights into the dynamics, including the ability to capture bubble breakup – a phenomenon that lies beyond the capabilities of the ROM. This study combines the ROM and the CFD simulations to predict spherical stability and breakup thresholds across varying bubble sizes, acoustic pressures, and frequencies. Three regimes are identified: (1) spherically stable bubbles, (2) stable surface mode oscillations, and (3) instability leading to breakup. The key finding is that the ROM reliably predicts breakup through unbounded growth of surface modes, demonstrating strong agreement with the results obtained from ALPACA simulations.

Keywords: bubble dynamics, direct numerical simulation, multiphase flow, sonochemistry, reduced order model

NOMENCLATURE

R_0	[μm]	initial bubble radius
R_E	[μm]	equilibrium bubble radius
T	[K]	temperature
$\hat{a}_n$	[−]	n^{th} dimensionless mode amplitude
a_n	[μm]	n^{th} mode amplitude
c	[m/s]	speed of sound
c_V	[J/K]	heat capacity at const. volume
f	[kHz]	excitation frequency
g_n	[m^2/s^2]	higher order terms
$l_{\max}$	[−]	max. number of refinements
p_0	[Pa]	ambient pressure
p_∞	[Pa]	stiffened gas EoS parameter
p_A	[Pa]	pressure amplitude
p_v	[Pa]	vapour pressure
t	[ms]	time
u	[m/s]	x-directional velocity
v	[m/s]	y-directional velocity
ϵ	[−]	small parameter
γ	[−]	stiffened gas EoS parameter
λ	[m]	wavelength
μ	[Pa · s]	dynamic viscosity
ω	[1/s]	angular frequency
ρ	[kg/m^3]	density
σ	[N/m]	coefficient of surface tension

Subscripts and Superscripts

B	bubble
B, 0	bubble, initial state
L	liquid

1. INTRODUCTION

The study of oscillating microbubbles in acoustic fields is a cornerstone of sonochemistry, where these bubbles play an important role in energy concentration that leads to chemical reactions [1, 2, 3, 4]. When subjected to acoustic excitation, microbubbles can undergo complex dynamics, including spherical oscillations, stable surface wave oscillations, bubble jetting [5, 6] and bubble breakup [7, 8]. Understanding these behaviors is crucial for scaling cavitation-driven chemical synthesis for industrial scales.

Copyright© Department of Fluid Mechanics, Budapest University of Technology and Economics and the Authors

A central challenge in modeling non-spherical microbubble oscillations lies in the uncertainty of both measurements and models. Experimental data for non-spherical oscillations are limited to a few parameter combinations [7, 9, 10], and they also often suffer from limitations in accuracy. Computational models must contend with assumptions and approximations that may not fully capture the complexity. To address these challenges, this study employs two complementary approaches: the reduced-order model (ROM) [11, 12, 13] and the high-fidelity ALPACA solver [14, 15]. The ROM provides a computationally efficient framework for analyzing radial bubble dynamics coupled with surface mode oscillations, making it suitable for large-scale parameter studies [16]. However, its validity is constrained to scenarios with small perturbations in surface modes [17]. In contrast, ALPACA is a compressible multiphase computational fluid dynamics (CFD) solver that solves the governing equations of fluid flow directly. Leveraging the level set method for interface capturing and a multiresolution meshing algorithm, ALPACA makes it possible to simulate surface mode oscillations and bubble breakup [18].

This study investigates the spherical stability and breakup limits of oscillating microbubbles by combining the strengths of ROM and ALPACA. A series of parameter studies is conducted to explore the effects of bubble size, pressure amplitude, and excitation frequency on bubble dynamics. ALPACA simulations are used to validate and refine ROM predictions. The second section discusses the ROM and the ALPACA solver. Then, the simulations are introduced in the third section and the results are discussed.

2. MODELING ACOUSTICALLY EXCITED BUBBLES

2.1. Reduced Order Model

The Reduced Order Model handles the non-spherical bubble dynamics as a vibration problem assuming axial symmetry and small deformation. The aim is to avoid partial differential equations by employing modal decomposition, specifically using Legendre polynomials as orthogonal basis functions, and to construct an ordinary differential equation system that describes the time evolution of the mode amplitudes. In this manner, the temporal evolution of the complex bubble shape r_s, expressed via Legendre polynomials as an infinite series in a spherical coordinate system that can be described as:

$$r_s(\theta, t) = R(t) + \sum_{n=2}^{\infty} \varepsilon a_n(t) P_n(\mu), \tag{1}$$

where $R(t)$ is the spherical or 0^{th} mode as the function of time, while a_n denotes the n^{th} mode amplitude corresponding to the Legendre polynomial $P_n(\mu)$ of order n, with $\mu = \cos(\mu)$. Note that the first mode, i.e., the translational motion, is neglected in this paper for simplicity. Additionally, surface distortion is assumed to be small, as indicated by the small parameter ε. Following the work of Shaw [11, 12, 13], the mode amplitudes are described by an implicit second-order nonlinear n-dimensional differential equation system derived from the Lagrangian function composed of the kinetic and potential energy. The nonlinear coupling terms permit interaction between the modes and account for the implicit nature of the system. The volume mode (the radial oscillation $R(t)$) reads as:

$$\left(1 - \frac{\dot{R}}{c_L}\right) R\ddot{R} + \left(1 - \frac{\dot{R}}{3c_L}\right) \frac{3}{2}\dot{R}^2 = G(t) + \frac{1}{c_L}\left(\dot{R} \cdot G(t) + R \cdot \dot{G}(t)\right) + \varepsilon^2 \left(g_0 + g_{0v}\right), \tag{2}$$

where c_L is the speed of sound in the liquid and

$$G(t) = \frac{p_{B_0}}{\rho_L}\left(\frac{R_0}{R}\right)^{3\gamma} + \frac{p_v}{\rho_L} - \frac{1}{\rho_L}\left(p_0 + p_A \sin(\omega t)\right) - \frac{4\mu_L \dot{R}}{\rho_L R} - \frac{2\sigma}{\rho_L R}. \tag{3}$$

In this context, p_{B_0} denotes the equilibrium pressure inside the bubble, while ρ_L represents the density of the liquid. The initial radius of the bubble is given by R_0, and γ refers to the ratio of specific heats. The dynamic viscosity of the liquid is denoted by μ_L, and σ stands for the surface tension. Acoustic excitation is characterized by the angular frequency ω and the pressure amplitude p_A. The ambient pressure, also known as the far-field pressure, is represented by p_0, and p_v indicates the vapour pressure. The higher order terms g_n and g_{nv} are the inviscid and damping terms, which can be found in [11, 12]. The surface modes have the following form:

$$\varepsilon \Big\{ R\ddot{a}_n + 3\dot{R}\dot{a}_n + \left[\left(n^2 - 1\right)(n+2)\frac{\sigma}{\rho_L R^2} - (n-1)\ddot{R}\right] a_n + \frac{2\mu_L}{\rho_L}\left[(n-1)(n+2)\frac{\dot{R}}{R^2}a_n + (n+2)(2n+1)\frac{\dot{a}_n}{R}\right]\Big\} = \varepsilon^2 \left(g_n + g_{nv}\right). \tag{4}$$

Like the 0^{th} mode, the second-order term governs the coupling between the modes, which can be separated into inviscid and damping components; the interested reader can find these terms in [16].

The solution strategy for the model is divided into two main parts: an initial value problem and a nonlinear equation system. The initial value problem is solved using a self-developed Runge–Kutta–Cash–Karp solver. At the same time, the nonlinear equation system is handled using a GPU-optimized iterative technique derived by the authors [16]. With this approach, the parameters of large spherical or closely spherically oscillating bubbles can be found efficiently. The deviation from the spherical shape is characterised by the mode ampli-

Copyright© Department of Fluid Mechanics, Budapest University of Technology and Economics and the Authors

tudes divided by the 0^{th} mode; from now on, relative mode amplitude $\hat{a}_n = a_n/R$. The approximated validity limit of the model, i.e., the maximum of the relative mode amplitude corresponding to the dominant mode (mode with the largest amplitude), is between 0.25 and 0.37 [17].

2.2. ALPACA Simulations

The CFD simulation of an oscillating microbubble in an acoustic field requires a compressible multiphase solver. The computational domain must span at least one wavelength to simulate a standing wave, which, in typical cases, is in the order of 10 mm, based on the speed of sound and excitation frequency. In contrast, bubble sizes in sonochemistry are typically around 10 µm, resulting in a scale difference of approximately three orders of magnitude. This significant disparity necessitates specialized numerical meshes.

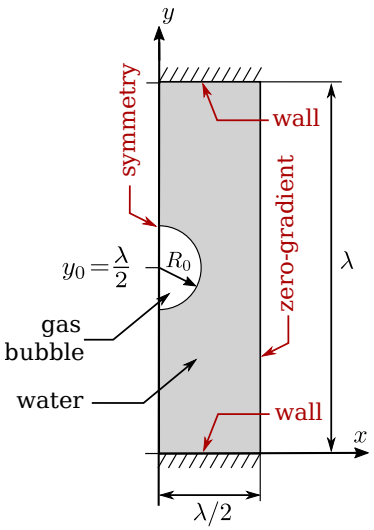

Figure 1. Layout and boundary conditions of the ALPACA simulations.

The chosen solver, ALPACA, meets these requirements, having been specifically developed to study compressible and multiphase phenomena [14]. ALPACA employs the level set method for interface capturing [19] and utilizes high-order, non-dissipative numerical schemes to accurately capture shockwaves [15]. Its meshing process is highly efficient, leveraging a multiresolution algorithm [20] that automatically refines the mesh as needed. The maximum number of refinements is controlled by the user defined parameter $l_{\max} \leq 14$, allowing the cell size to vary by nearly four orders of magnitude.

ALPACA was used to carry out two-dimensional axisymmetric numerical simulations of bubbles in a standing wave. The bubble was positioned at the node of the acoustic standing wave within a rectangular domain of dimensions $\lambda \times \lambda/2$, where λ represents the wavelength. The boundary conditions are illustrated in Figure 1. Reflective walls were placed on the south and north boundaries, causing wave reflections. A zero-gradient boundary condition was applied on the east boundary, while the west boundary served as the axis of symmetry. The standing wave was introduced through the initial conditions, and the bubble was subjected to the following pressure:

$$p(t) = p_0 - p_A \cdot \sin(2\pi f \cdot t). \tag{5}$$

The initial conditions in the bubble correspond to the equilibrium condition, that is

$$p_B(x, y) = p_0 + \frac{2\sigma}{R_0}, \tag{6}$$

where p_B is the bubble pressure, σ is the surface tension and R_0 corresponds to the equilibrium radius. The initial velocities are zero and the density is set according to the ideal gas law:

$$u_B(x, y) = 0, \tag{7}$$

$$v_B(x, y) = 0 \text{ and} \tag{8}$$

$$\rho_B(x, y) = \frac{p_B(x, y)}{(\gamma_B - 1)c_V T_B}, \tag{9}$$

where u_B is the x-directional velocity, v_B is the y-directional velocity and ρ_B is the density in the bubble. In both phases, the stiffened gas equation of state is used [21]:

$$p = (\gamma - 1)\rho e - p_\infty, \tag{10}$$

where e is the internal energy and γ, p_∞ are parameters. In the gas phase $p_{\infty,B} = 0$, thus the stiffened gas EoS results in the ideal gas law, in which $\gamma_B = 1.4$ is the ratio of specific heats. To model the water, parameters $\gamma_L = 4.4$ and $p_{\infty,L} = 6 \cdot 10^8$ Pa are adopted from the literature [22].

To accelerate the formation of surface mode oscillations, the bubble shape is initially perturbed with relative mode amplitudes of $\hat{a}_2 = 0.031$, $\hat{a}_3 = -0.050$, $\hat{a}_4 = 0.008$, and $\hat{a}_5 = 0.016$. These amplitudes are chosen to ensure that the volume of the bubble remains unchanged. A post-processing code was developed in Paraview to extract the mode amplitudes from the numerical simulations.

In total, 62 ALPACA simulations were conducted, with each simulation running for 24 hours on the SUPERMUC-NG supercomputer, utilizing one compute node with 36 cores. In most cases, this computing time was sufficient to run the simulations for at least 10 acoustic cycles, enabling the analysis of long-term behavior. For lower frequencies, simulating the same number of acoustic cycles requires more time, as the period of the oscillation is longer, and more time steps are necessary. Simulating smaller bubbles necessitates a reduction in cell size, and in accordance with the CFL condition, the time step size is also reduced. To account for these factors, the simulations were extended for an additional 24 hours compute time in the case of low frequencies and small bubbles.

3. SIMULATION RESULTS

This section presents the results of the ALPACA and ROM simulations. First, the convergence of the

Copyright© Department of Fluid Mechanics, Budapest University of Technology and Economics and the Authors

ALPACA simulations is analyzed by increasing the mesh resolution and comparing the results to ROM predictions. Next, the frequency and bubble radius are fixed to investigate the effect of pressure amplitude, and the classification of surface modes are discussed. Finally, large-scale parameter studies are introduced.

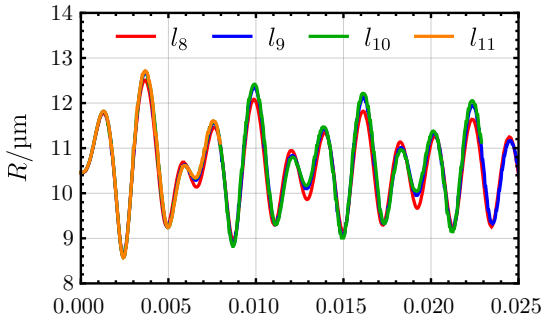

(a) Radius

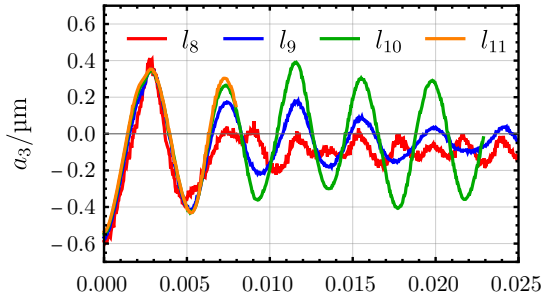

(b) 3rd mode

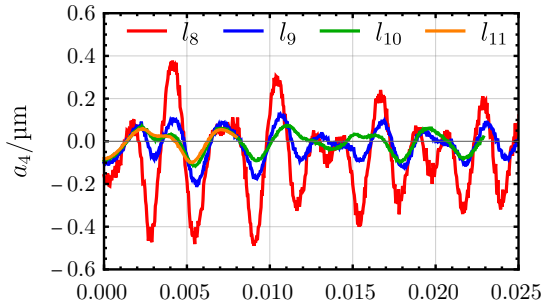

(c) 4th mode

Figure 2. Results of the convergence study with parameters $R_0 = 10.5\,\mu m$, $p_A = 50\,kPa$ and $f = 480\,kHz$.

3.1. Mesh independence study of ALPACA

A bubble with an initial radius of $R_0 = 10.5\,\mu m$ is excited by a standing wave with an amplitude of $p_A = 50\,kPa$ and a frequency of $f = 480\,kHz$. According to the ROM, a stable 3rd mode oscillation is expected to form. Simulations were conducted in ALPACA using four different mesh resolutions. The number of adaptive refinements was varied from 8 to 11 on an initial 80×144 mesh. This resulted in the number of cells along the bubble diameter being $N_{bubble} = 76, 152, 304$, and 608 for the resolutions l_8, l_9, l_{10}, and l_{11}, respectively. Figure 2a demonstrates that the l_9 mesh already produces accurate results in the bubble radius, as further increase of the resolution does not lead to significant changes. Figures 2b and 2c illustrate the 3rd and 4th modes, respectively.

In the figures, clear convergence is visible. Using the l_{10} mesh, the desired 3rd mode oscillation forms with an amplitude of $a_3 \approx 0.3\,\mu m$, while the 4th mode dampens to $a_4 \approx 0.05\,\mu m$. For comparison, the ROM predicts $a_3 = 0.297\,\mu m$ and $a_4 = 0.023\,\mu m$. Based on these results, a mesh resolution of $N_{bubble} \approx 300$ is used for all subsequent ALPACA simulations.

3.2. Effect of pressure amplitude

The effect of increasing pressure amplitude is examined for a bubble with an initial radius of $R_0 = 47.5\,\mu m$ excited by a frequency of $f = 30\,kHz$ acoustic standing wave at various pressure amplitudes in ALPACA. According to the ROM, the bubble remains spherical when the pressure amplitude p_A is below 19 kPa. For pressure amplitudes exceeding 39 kPa, unstable surface mode oscillations occur ($a_n \to \infty$), potentially leading to bubble breakup. In the intermediate range, $19\,kPa < p_A < 39\,kPa$, stable 2nd and 3rd mode oscillations develop. The radius–time curves in Figure 3 depict the radial dynamics in selected ALPACA simulations, showing remarkable agreement between the ALPACA simulations (red line) and the ROM predictions (black dashed line). The mode amplitude–time curves are presented for the same ALPACA simulation in Figure 4. The formation of stable surface mode oscillations takes hundreds of acoustic periods in the ROM; thus, it cannot be compared directly with ALPACA. The following observations can be made:

1. For a low pressure amplitude ($p_A = 10\,kPa$) the initial perturbation in the modes damps down as illustrated in Figure 4a. The bubble is considered spherically stable in that case. This point falls below the spherical stability limit, aligning with the ROM results.

2. For pressure amplitudes $p_A = 32\,kPa$ and $p_A = 36\,kPa$, there is an initial large 3rd mode oscillation observed during the first few acoustic cycles as depicted in Fig. 4b. However, this dampens down and a stable 2nd mode oscillation remains. The ROM predicts a dominant 2nd mode for $p_A = 32\,kPa$, and a dominant 3rd mode for $p_A = 36\,kPa$ that differs from ALPACA results as depicted in Fig. 4c.

3. For a high pressure amplitude ($p_A = 42\,kPa$), the initial perturbation grows, leading to bubble breakup at 0.072 ms. This breakup event is indicated by a vertical dashed line in Figs. 3d and 4d. For this particular parameter combination the ROM predicts diverging mode amplitudes ($a_n \to \infty$).

Copyright© Department of Fluid Mechanics, Budapest University of Technology and Economics and the Authors

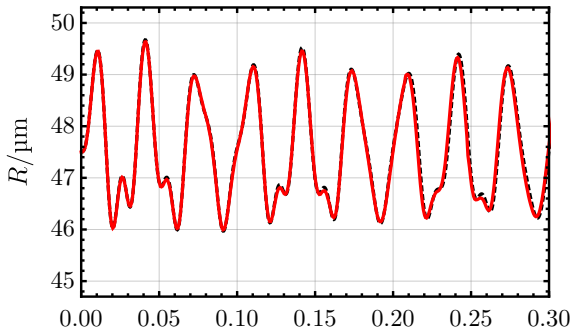

(a) $p_A = 10\,\mathbf{kPa}$

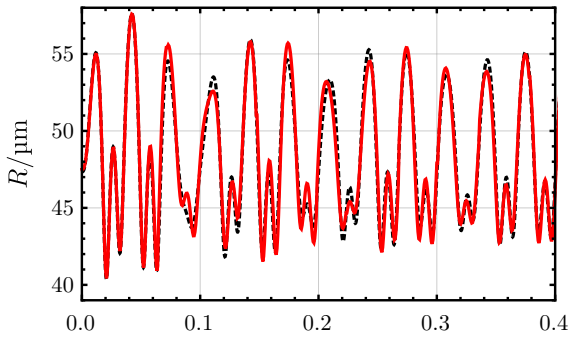

(b) $p_A = 32\,\mathbf{kPa}$

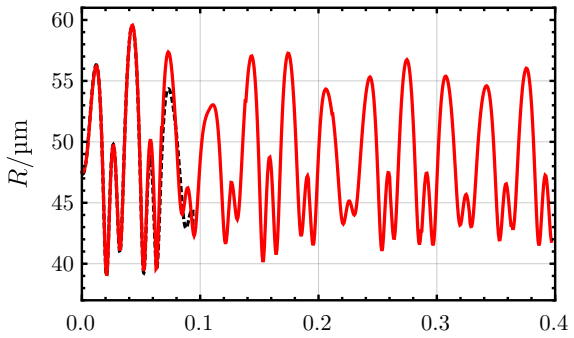

(c) $p_A = 36\,\mathbf{kPa}$

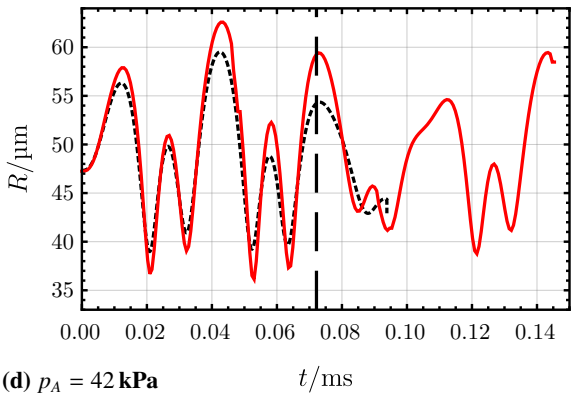

(d) $p_A = 42\,\mathbf{kPa}$

Figure 3. Radius over time for a $R_0 = 47.5\,\mu\mathbf{m}$ bubble excited with $f = 30\,\mathbf{kHz}$ ultrasound. (black dashed: ROM)

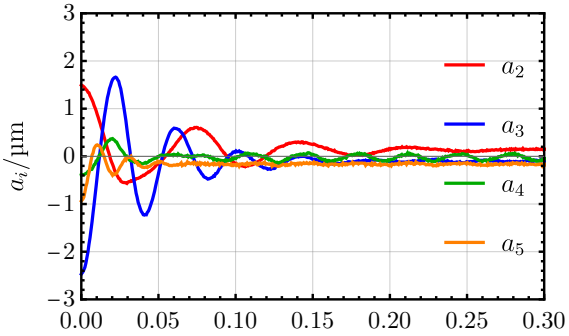

(a) $p_A = 10\,\mathbf{kPa}$

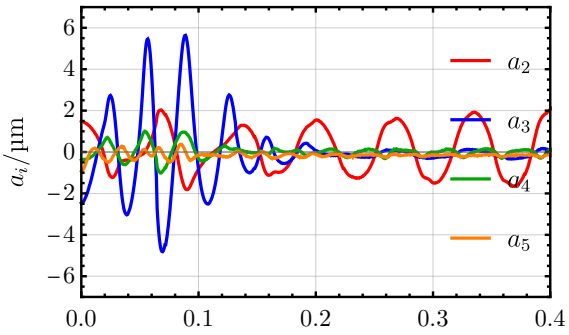

(b) $p_A = 32\,\mathbf{kPa}$

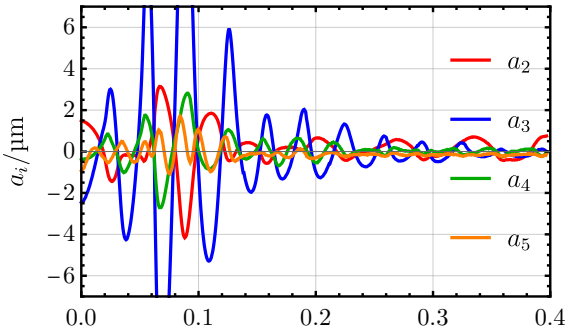

(c) $p_A = 36\,\mathbf{kPa}$

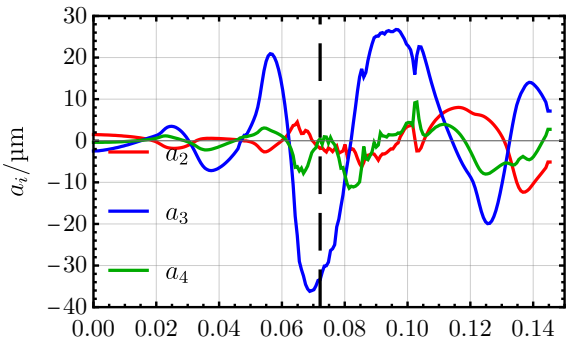

(d) $p_A = 42\,\mathbf{kPa}$

Figure 4. Mode amplitudes over time for a $R_0 = 47.5\,\mu\mathbf{m}$ bubble excited with $f = 30\,\mathbf{kHz}$ ultrasound.

Copyright© Department of Fluid Mechanics, Budapest University of Technology and Economics and the Authors

The results indicate that the ALPACA simulations and the ROM predict similar spherical stability and breakup limits. Based on the simulations, the spherical stability limit in ALPACA is between 10 kPa $< p_A <$ 25 kPa, compared to $p_A = 19$ kPa in the ROM. Similarly, the breakup limit in ALPACA lies between 36 kPa $< p_A <$ 42 kPa, while the ROM predicts diverging mode amplitudes above $p_A = 39$ kPa. That indicates that diverging mode amplitudes in ROM can be a sign of bubble breakup.

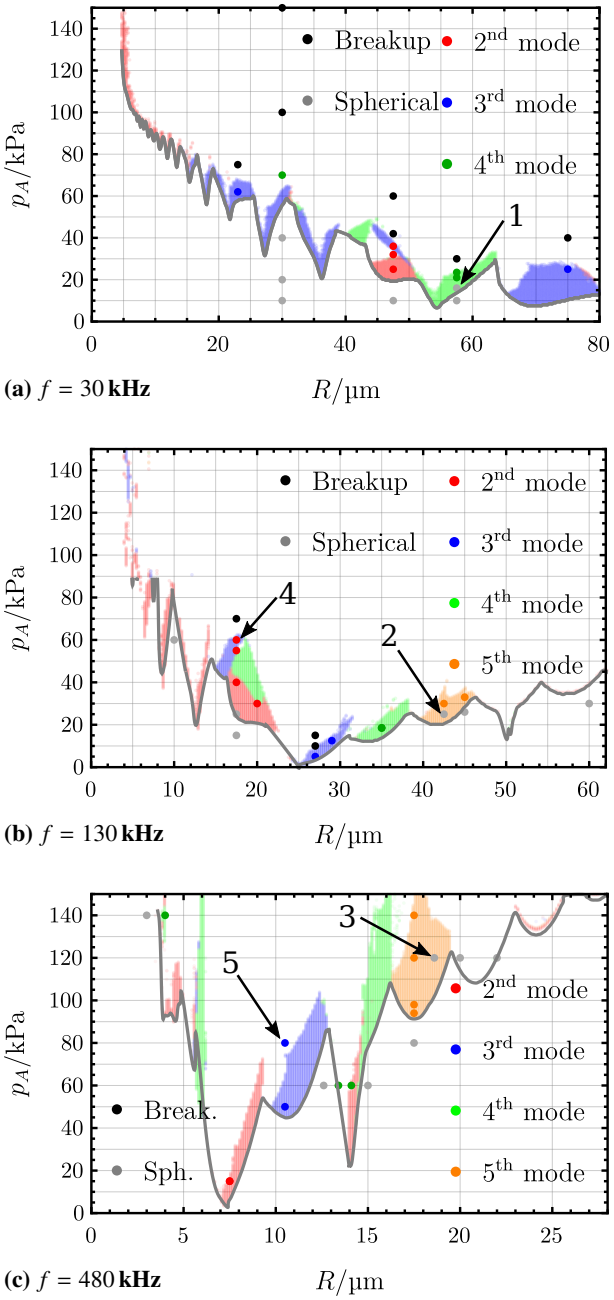

(a) $f = 30$ **kHz**

(b) $f = 130$ **kHz**

(c) $f = 480$ **kHz**

Figure 5. Parameter studies at various frequencies, the background is colored based on the ROM results, the dots show the ALPACA results. The gray line indicates the limit of stability (in ROM).

3.3. Parameter studies

Three parameter studies were conducted using the ROM. In each parameter study, the frequency was held constant while the bubble radius and pressure amplitude were adjusted in the ranges specified in Table 1. The dominant mode (i.e., the mode with the largest amplitude) was identified in each case. If the dominant mode amplitude does not reach $\hat{a}_n = 0.001$, then the bubble is considered spherically stable.

Table 1. Parameters used in the studies

Frequency	f	30 kHz/130 kHz/480 kHz
Equiv. radius	R_E	0 µm . . . 80 µm
Pressure ampl.	p_A	0 kPa . . . 150 kPa

The dominant modes are plotted in the (R, p_A) plane for the $f = 30$ kHz, 130 kHz and 480 kHz cases in Figures 5a, 5b and 5c, respectively. The various colors correspond to the different modes, as indicated in the legend. The gray line shows the limit of spherical stability, below which the bubble is considered spherical according to the ROM. Above the spherical stability line, where there is no color in the plot the bubble undergoes breakup. ALPACA simulations were carried out for selected cases, marked by dots based on the dominant mode amplitude. Below the spherical stability limit, as determined by the ROM (gray line), the bubbles in ALPACA also exhibit spherical stability. Slightly above the stability limit, the surface mode oscillations remain small and cannot be seen in the ALPACA simulations. For instance, in Fig. 5a in point marked by 1, the modes amplitudes are so small that they cannot be resolved by ALPACA with the given mesh resolution.

The stable surface mode oscillations generally show good agreement between the ROM and the ALPACA simulations. However, there are some cases where discrepancies occur, particularly for higher surface modes, as exemplified in Fig. 5b in point 2, and Fig. 5c in point 3. Additionally, cases with high surface mode amplitudes above the validity limit of ROM can also exhibit differences, such as $\hat{a}_2 > 0.3$ in Fig. 5b in point 4. It is important to note that bubble breakup consistently occurs above the region of stable surface oscillations. However, there are instances where the bubble does not break up, although predicted by the ROM (e.g., Fig. 5c point 5). This can be attributed to the validity limit, as it assumes small perturbations in the surface and may not accurately capture the behavior in cases with significant surface perturbations.

Out of the 62 ALPACA simulations, 54 of them (87%), qualitatively align with the ROM predictions. The simulation results are summarized in Tables 2, 3 and 4 in the Appendix. Based on these observations, it can be concluded that the spherical stability limit and the stable surface mode oscillations are accurately predicted by the reduced order model, as long as the validity limit of the ROM is not exceeded. The

Copyright© Department of Fluid Mechanics, Budapest University of Technology and Economics and the Authors

approximated validity limit of the model is between $0.25 < \hat{a}_n < 0.37$ [17]. Furthermore, the ALPACA simulations verify that diverging mode amplitudes in ROM can indicate bubble breakup in some cases.

4. CONCLUSION

This study presents a comprehensive comparison of the ALPACA and ROM models for predicting surface oscillations and bubble breakup in oscillating microbubbles. The results demonstrate a high level of agreement between the two approaches, with ALPACA and ROM predictions aligning in 87% of cases. The ALPACA simulations achieved accurate results using a bubble resolution of $N_{\text{bubble}} \approx 300$. Deviations between the models were observed primarily in scenarios where the surface mode oscillations were small, and could not be resolved in ALPACA with the applied resolution, or when the dimensionless mode amplitudes exceeded the validity limit of the ROM.

In conclusion, the two models predict similar spherical stability and breakup limits, highlighting their reliability for simulating bubble dynamics. The results demonstrate that diverging mode amplitudes in ROM can effectively indicate bubble breakup, even when these amplitudes exceed its validity limit. This finding means that ROM could be a computationally effective method to identify bubble breakup, although flow simulations with ALPACA provide more details for capturing high-amplitude surface mode oscillations and bubble breakup. Together, these models offer complementary insights into the stability and breakup phenomena of oscillating microbubbles.

ACKNOWLEDGEMENTS

This research was supported by the EKÖP, Hungary funded by the National Research Development and Innovation Fund under grant number EKÖP-24-3-BME-84. The authors gratefully acknowledge the Gauss Centre for Supercomputing e.V. (www.gauss-centre.eu) for funding this project by providing computing time on the GCS Supercomputer SuperMUC-NG at Leibniz Supercomputing Centre (www.lrz.de). Project no. TKP-6-6/PALY-2021 has been implemented with the support provided by the Ministry of Culture and Innovation of Hungary from the National Research, Development and Innovation Fund, financed under the TKP2021-NVA funding scheme. The authors acknowledge the financial support of the Hungarian National Research Development and Innovation Office via NKFIH grants OTKA FK142376 and OTKA PD142254.

APPENDIX A

Tables 2, 3 and 4 contain all the ALPACA simulation parameters and the identified dominant mode in ALPACA and the ROM.

Table 2. Comparison at $f = 30$ kHz

R/μm	p_A/kPa	Dominant mode ALPACA	Dominant mode ROM
47.5	10	none	none
47.5	25	2	2
47.5	32	2	2
47.5	36	2	3
47.5	42	breakup	breakup
47.5	60	breakup	breakup
75	25	3	3
75	25	breakup	breakup
57.5	10	none	none
57.5	16	none	4
57.5	21	4	4
57.5	23.5	4	4
57.5	30	breakup	breakup
23	62	3	3
23	75	breakup	breakup
30	10	none	none
30	10	none	none
30	10	none	none
30	10	4	breakup
30	10	breakup	breakup
30	10	breakup	breakup

Table 3. Comparison at $f = 130$ kHz

R/μm	p_A/kPa	ALPACA	ROM
17.5	15	none	none
17.5	25	none	none
17.5	40	2	2
17.5	55	2	3
17.5	60	2	3
17.5	70	breakup	breakup
27	5	3	3
27	10	breakup	breakup
27	15	breakup	breakup
45	26	none	none
20	30	2	2
29	12.5	3	3
35	18.5	4	4
42.5	25	none	5
42.5	30	5	5
45	33	5	5
10	60	none	none
60	30	none	none

Table 4. Comparison at $f = 480$ kHz

R/μm	p_A/kPa	ALPACA	ROM
17.5	80	none	none
17.5	94	5	5
17.5	98	5	5
17.5	120	5	5
17.5	140	5	5
18.6	120	none	5
20	120	none	none
22	120	none	none
10.5	50	3	3
10.5	80	3	break
7.5	15	2	2
12.6	60	none	none
13.4	60	4	break
14.1	60	4	2
15	60	none	none
3	140	none	none
3	140	4	4
30	10	none	none
30	20	none	none
30	40	none	none
30	70	none	none
30	100	none	none
30	150	none	none

Copyright© Department of Fluid Mechanics, Budapest University of Technology and Economics and the Authors

REFERENCES

[1] Sochard, S., Wilhelm, A., and Delmas, H., 1997, "Modelling of free radicals production in a collapsing gas-vapour bubble", *Ultrasonics Sonochemistry*, Vol. 4 (2), pp. 77–84.

[2] Kubicsek, F., Kozák, Á., Turányi, T., Zsély, I. G., Papp, M., Al-Awamleh, A., and Hegedûs, F., 2024, "Ammonia production by microbubbles: A theoretical analysis of achievable energy intensity", *Ultrasonics Sonochemistry*, Vol. 106, p. 106876.

[3] Cho, S., and Yun, S. H., 2020, "Structure and optical properties of perovskite-embedded dual-phase microcrystals synthesized by sonochemistry", *Communications Chemistry*, Vol. 3 (1), pp. 1–7.

[4] Al-Awamleh, A., and Hegedűs, F., 2024, "Sono-hydrogen: a Theoretical Investigation of its Energy Intensity", *Periodica Polytechnica Mechanical Engineering*, Vol. 68 (3), pp. 254–263.

[5] Rosselló, J., Lauterborn, W., Koch, M., Wilken, T., Kurz, T., and Mettin, R., 2018, "Acoustically induced bubble jets", *Physics of Fluids*, Vol. 30 (12).

[6] Prabowo, F., and Ohl, C.-D., 2011, "Surface oscillation and jetting from surface attached acoustic driven bubbles", *Ultrasonics sonochemistry*, Vol. 18 (1), pp. 431–435.

[7] Versluis, M., Goertz, D. E., Palanchon, P., Heitman, I. L., van der Meer, S. M., Dollet, B., de Jong, N., and Lohse, D., 2010, "Microbubble shape oscillations excited through ultrasonic parametric driving", *Physical review E*, Vol. 82 (2), p. 026321.

[8] Mur, J., Reuter, F., Agrež, V., Ohl, C.-D., et al., 2024, "Optic generation and perpetuation of acoustic bubble clusters", *Ultrasonics Sonochemistry*, Vol. 110, p. 107023.

[9] Guédra, M., and Inserra, C., 2018, "Bubble shape oscillations of finite amplitude", *Journal of Fluid Mechanics*, Vol. 857, pp. 681–703.

[10] Cleve, S., Guédra, M., Mauger, C., Inserra, C., and Blanc-Benon, P., 2019, "Microstreaming induced by acoustically trapped, non-spherically oscillating microbubbles", *Journal of Fluid Mechanics*, Vol. 875, pp. 597–621.

[11] Shaw, S. J., 2006, "Translation and oscillation of a bubble under axisymmetric deformation", *Physics of Fluids*, Vol. 18 (7), p. 072104.

[12] Shaw, S. J., 2009, "The stability of a bubble in a weakly viscous liquid subject to an acoustic traveling wave", *Physics of Fluids*, Vol. 21 (2), p. 022104.

[13] Shaw, S. J., 2017, "Nonspherical submillimeter gas bubble oscillations: Parametric forcing and nonlinear shape mode coupling", *Physics of Fluids*, Vol. 29 (12), p. 122103.

[14] Hoppe, N., Adami, S., and Adams, N. A., 2022, "A parallel modular computing environment for three-dimensional multiresolution simulations of compressible flows", *Computer Methods in Applied Mechanics and Engineering*, Vol. 391, p. 114486.

[15] Hoppe, N., Winter, J. M., Adami, S., and Adams, N. A., 2022, "ALPACA - a level-set based sharp-interface multiresolution solver for conservation laws", *Computer Physics Communications*, Vol. 272, p. 108246.

[16] Kalmár, P., Hegedűs, F., Nagy, D., Sándor, L., and Klapcsik, K., 2023, "Memory-friendly fixed-point iteration method for nonlinear surface mode oscillations of acoustically driven bubbles: from the perspective of high-performance GPU programming", *Ultrasonics Sonochemistry*, Vol. 99, p. 106546.

[17] Kalmár, P., Hegedűs, F., and Klapcsik, K., 2024, "A comparative study of measurements and numerical simulations of acoustically excited non-spherical bubbles oscillation", *International Journal of Multiphase Flow*, Vol. 179, p. 104947.

[18] Nagy, D., and Hegedűs, F., 2023, "Az ALPACA szoftver validációja akusztikusan gerjesztett gázbuborékok szimulációjára: Validation of ALPACA for the simulation of acoustically excited gas bubbles", *Nemzetközi Gépészeti Konferencia–OGÉT*, pp. 360–365.

[19] Osher, S., and Fedkiw, R. P., 2001, "Level set methods: an overview and some recent results", *Journal of Computational physics*, Vol. 169 (2), pp. 463–502.

[20] Harten, A., 1995, "Multiresolution algorithms for the numerical solution of hyperbolic conservation laws", *Communications on Pure and Applied Mathematics*, Vol. 48 (12), pp. 1305–1342.

[21] Harlow, F. H., and Amsden, A. A., 1971, "Fluid Dynamics. A LASL Monograph.", *Tech. rep.*, Los Alamos National Lab.(LANL), Los Alamos, NM (United States).

[22] Kaiser, J. W., Hoppe, N., Adami, S., and Adams, N. A., 2019, "An adaptive local time-stepping scheme for multiresolution simulations of hyperbolic conservation laws", *Journal of Computational Physics*, Vol. 4, p. 100038.

Copyright© Department of Fluid Mechanics, Budapest University of Technology and Economics and the Authors